



Green photocatalytic synthesis of vitamin B₃ by Pt loaded TiO₂ photocatalysts



Sedat Yurdakal^{a,*}, Şadiye Özge Yanar^a, Sıdıka Çetinkaya^a, Oğuzhan Alagöz^b, Pınar Yalçın^a, Levent Özcan^c

^a Kimya Bölümü, Fen-Edebiyat Fakültesi, Afyon Kocatepe Üniversitesi, Ahmet Necdet Sezer Kampüsü, 03200 Afyonkarahisar, Turkey

^b Kimya Mühendisliği Bölümü, Mühendislik Fakültesi, Afyon Kocatepe Üniversitesi, Ahmet Necdet Sezer Kampüsü, 03200 Afyonkarahisar, Turkey

^c Biyomedikal Mühendisliği Bölümü, Mühendislik Fakültesi, Afyon Kocatepe Üniversitesi, Ahmet Necdet Sezer Kampüsü, 03200 Afyonkarahisar, Turkey

ARTICLE INFO

Article history:

Received 19 July 2016

Received in revised form

19 September 2016

Accepted 26 September 2016

Available online 28 September 2016

Authors dedicate this article to the retirement and to the career of Prof. Vincenzo Augugliaro (Palermo University, Italy).

Keywords:

Vitamin B₃

Photocatalysis

Green synthesis

Pt loaded TiO₂

pH effect

ABSTRACT

Selective photocatalytic oxidation of 3-pyridinemethanol to 3-pyridinemethanal and vitamin B₃ by using pristine and Pt loaded home prepared (HP) rutile and commercial TiO₂ photocatalysts, under UV, UV-vis and visible irradiations in water, was performed in friendly environmental conditions. The photocatalysts were characterized by XRD, SEM-EDAX, BET, DRS, XPS and TGA techniques. The influence of pH on reactivity and total selectivity to 3-pyridinemethanol and vitamin B₃ was studied. Under very acidic conditions (pH = 2) no or low activity (depending on photocatalyst) was observed, whereas by increasing the pH from 4 to 12 very high total selectivity was achieved. The Pt loading was beneficial for selectivity whereas the reactivity was positively affected only for crystalline HP sample. This last sample showed good activity under visible irradiation, exhibiting an about 4 times higher conversion than the other samples. The influence of the position of the benzylic group in pyridine (2-pyridinemethanol and 4-pyridinemethanol) was also studied. The results showed that to synthesize vitamin B₃ in green conditions the photocatalyst should be poorly crystalline or Pt loaded.

© 2016 Elsevier B.V. All rights reserved.

1. Introduction

Heterogeneous photocatalysis by TiO₂ fulfills the principles of Green Chemistry as the experiments are generally carried out in water at ambient temperature and under sunlight by using oxygen from air as the oxidant [1]. A semiconductor such as TiO₂ is very suitable for green photocatalysis as it is very effective, cheap and stable to photocorrosion [2]. Using oxygen from air without doing any purification is very simple, economic and hazardless. Water is also very cheap, sustainable and un-flammable solvent [3]. By considering that fossil fuels will end near future, using sunlight as energy source becomes a very important challenge for mankind. In addition, working at room temperature and pressure decreases energy requirement and costs for reactor security.

Heterogeneous photocatalysis has been mainly employed to oxidise organic and inorganic pollutants in liquid or gaseous phases

[2]. The oxidation reaction in water, due mainly to primary oxidant species as hydroxyl radicals, has been considered unselective and therefore synthesis reactions generally have been carried out in organic solvents [4]. Photocatalytic selective oxidation of benzyl alcohol derivatives [5], 5-(hydroxymethyl)-2-furaldehyde [6], amines [7], piperonyl alcohol [8], *trans*-ferulic acid [9], isoeugenol [10], and glycerol [11] or selective cyclization of aromatic acids [12] are examples of synthetic reactions performed in water.

It is well known that Pt loading of TiO₂ photocatalysts increases the activity both under UV and visible irradiation [7,12]; in fact Pt loading decreases the electron-hole recombination rate and therefore the reaction rate increases. By using metal loaded TiO₂, photocatalytic reactions under visible or sunlight irradiation have been generally performed for degrading harmful compounds [13], some investigations having been also carried out to perform organic syntheses in organic solvents [14]. For instance photocatalytic oxidation of aniline to nitrosobenzene has been selectively (90%) performed by using Pt-loaded TiO₂ in toluene and under visible irradiation [14c].

Vitamin B₃ (pyridine-3-carboxylic acid), whose world production is around 35,000 tons per year [15], is generally used in the

* Corresponding author.

E-mail addresses: sedatyurdakal@gmail.com, syurdakal@aku.edu.tr
(S. Yurdakal).

prevention and treatment of pellagra disease. Industrially vitamin B₃ and other pyridine carboxylic acids are produced at high pressure by oxidation of picolinic isomers using nitric acid, permanganate or chromic acid and vanadia-titania-zirconia oxide supported catalysts [15]. Just three research papers were published on the photocatalytic selective oxidation of 3-pyridine-methanol [16,17] and its derivatives [15] to their corresponding aldehydes and acids. These reactions were performed in water, under acidic conditions (pH 1–4) [15–17] and using commercial TiO₂ [15,17] and TiO₂-graphene-like [16] composite photocatalysts. In addition, the reactions were performed under de-aerated conditions using cupric ions as electron acceptor in order to minimize the electron-hole recombination. pH and temperature influence on 3-pyridine-methanol oxidation was also investigated [15]. It was found that temperature effect was negligible for products yields while, by increasing pH from 1 to 4, both aldehyde and vitamin B₃ yields and Cu²⁺ ions conversion decreased. In these works, high total selectivity values were obtained, being selectivities to aldehyde higher than those to acid. Selective production of pyridinecarboxaldehydes from methylpyridine isomers was also performed under de-aerated conditions in acetonitrile or acetonitrile-water solvents [18]. The obtained results show that the reactivity is strongly dependent on the photocatalyst properties.

In our recent work selective photocatalytic oxidation of 4-methoxybenzyl alcohol and 4-nitrobenzyl alcohol was performed in water under simulated solar light by using Pt, Au, Pd and Ag loaded Degussa P25 TiO₂ catalysts [19]. The best activity and selectivity results were obtained with Pt-loaded (0.5%) TiO₂ and the highest aldehyde selectivities were reached at low pH's. Significant amount of 4-nitrobenzoic acid (*ca.* 50%) was obtained only from 4-nitrobenzyl alcohol at high pH values.

In this work, differently from the previously cited works [15–17,19], Pt-loaded home prepared (HP) TiO₂ photocatalysts were used for selective oxidation of 2, 3 and 4-pyridinemethanol to its corresponding aldehyde and acid in water. Oxygen from atmospheric air was used as oxidant; the influence of different light sources (UV, UV-vis and visible) on substrate degradation rates and products selectivities was also investigated for different pH's (2–12). The optimal amount to be loaded on TiO₂ was already investigated [19] and this amount (0.5%) has been used for the TiO₂ samples of this work.

2. Experimental

2.1. Preparation of photocatalysts

2.1.1. Preparation of HPRT

The precursor solution was obtained by adding 20 mL of TiCl₄ to 1000 mL of water contained in a volumetric flask (2 L). At the end of the addition, the resulting solution was stirred for 2 min by a magnetic stirrer and then the flask was sealed and maintained at room temperature (*ca.* 298 K) for a total aging time of 6 days. After that time the precipitated powder was separated by decantation and dialysed several times with deionised water until a neutral pH was reached. Then, the sample was centrifuged and dried at room temperature. The final HP catalyst is hereafter indicated as HPRT [6]. A thermal treated HPRT sample was prepared by calcining it for 3 h at 400 °C (HPRT-400).

2.1.2. Preparation of 0.5% Pt loaded samples: Pt-P25, Pt-HPRT and Pt-HPRT-400

The details of metal loading on TiO₂ by photoreduction method are reported elsewhere [19]. 2 L of water, 500 mL of ethanol (as reductive agent), 10 g of TiO₂ (P25, HPRT or HPRT-400) and a nom-

inal amount of Pt (50 mL of 1 ppm Pt aqueous solution of PtCl₄) were mixed together. This suspension was ultrasonicated for 15 min.

A Pyrex batch photoreactor of cylindrical shape, with volume of 2.5 L, was used for photodeposition of Pt on suspended TiO₂ by photoreduction of Pt cations. The photoreactor was provided with ports in its upper section for the inlet and outlet of gases. A magnetic bar guaranteed a satisfactory suspension of the photocatalyst and the uniformity of the reacting mixture. A 700 W medium pressure Hg lamp (Helios Italquartz) was axially immersed within the photoreactor and it was cooled by water circulating through a Pyrex thimble; the temperature of the suspension was about 300 K. The aqueous solution was deaerated by bubbling He at atmospheric pressure for 30 min in the dark and then the lamp was turned on. The gas was continuously bubbled during the photodeposition that lasted 8 h. Then it was waited until the metal loaded TiO₂ was precipitated; the solid phase was separated by decantation. The resulting powder was washed two times by using 2.5 L of deionised water. Lastly the powder was dried at room temperature for obtaining fine powders hereafter called Pt-HPRT and Pt-HPRT-400. Pt-loaded P25 sample was calcined at 400 °C (Pt-P25).

2.2. Characterization

XRD patterns of the powders were recorded by Bruker D8 Advance diffractometer using the Cu K α radiation and a 2θ scan rate of 1.281°/min.

SEM images were obtained using an ESEM microscope (FEI Nova Nano Sem 650) with Through Lens Detector (TLD) and/or Coherence Backscattering Detector (CBS). BET specific surface areas were measured by the multi-point BET method using a Micromeritics (Gemini 2360 model) apparatus. Before the measurement, the samples were outgassed for 3 h at 250 °C. Thermogravimetric analysis (TGA) was performed by using Shimadzu equipment (model TG60H). The heating rate was 10 °C/min in N₂ atmosphere and the used powder amount was *ca.* 8 mg. Ultraviolet-visible spectra were obtained in the 300–800 nm range by diffuse reflectance spectroscopy by using a Shimadzu UV-2401 PC instrument with BaSO₄ as the reference.

X-ray photoelectron spectroscopy (XPS) measurements were carried out by using a Thermo Fischer K-Alpha spectrometer. All the binding energies were referred to the C 1 s peak at 284.6 eV.

¹H NMR spectra was recorded on a Varian Mercury-400 High Performance Digital FT-NMR spectrometer. Chemical shifts are reported in ppm. DMSO (δ = 2.50 ppm) was used as a solvent and tetramethylsilane was used as the internal standard.

2.3. Photoreactivity setup and procedure

The details of photoactivity set-up and procedure are reported elsewhere [20]. A cylindrical Pyrex batch photoreactor, containing 150 mL of aqueous suspension, was used to perform the reactivity experiments under UV-vis irradiation. The photoreactor was provided with an immersed lamp and with open ports in its upper section for contacting the suspension with atmospheric air and for sampling. A magnetic stirrer guaranteed a satisfactory suspension of the photocatalyst and the homogeneity of the reacting mixture. A 100 W halogen lamp (Osram, Germany) was axially positioned within the photoreactor; it was cooled by water circulating through a Pyrex thimble surrounding the lamp. In order to perform the experiments under visible irradiation, the circulating liquid was 1 M NaNO₂ aqueous solution, which totally prevented UV irradiation from reaching the suspension.

For the runs carried out under UV radiation a continuously stirred beaker (volume: 250 mL; diameter: 6.7 cm) containing 150 mL of aqueous suspension was used as photoreactor. In this case the suspension was irradiated by four fluorescent lamps

Table 1

Features of the light sources.

Light source	Light irradiance 315–400 nm (mW cm ⁻²)	Light irradiance 400–1050 nm (mW cm ⁻²)	Reactor geometry
UV-vis	1.3	197	Annular
UV	2.1	—	Cylindrical
Visible	—	197	Annular

(Philips, 8 W) emitting at 365 nm. These lamps were positioned at a distance of 6.8 cm from the top of the suspension. The average values of the radiation energy impinging on the suspension (for UV system) or transmitted at the external surface of the reactor in the absence of catalyst (for UV-vis and visible systems) were measured by using a radiometer (Delta Ohm, DO 9721). These values are reported in Table 1 for the different radiation sources. All the experiments were carried out at room temperature.

Preliminary reactivity tests, carried out both with 3-pyridinemethanol and 3-pyridinemethanal, showed that the contemporary presence of catalyst, radiation and oxygen was necessary for the occurrence of substrate oxidation. For all the photocatalytic runs the substrate initial concentration and the catalyst amount were 0.50 mM and 0.20 g L⁻¹, respectively. Before switching on the lamp, the suspension was stirred for 30 min at room temperature in order to reach the thermodynamic equilibrium. During the runs samples of reacting suspension were withdrawn at fixed time intervals; they were immediately filtered through a 0.45 µm hydrophilic membrane (HA, Millipore) before being analysed.

The quantitative determination and identification of the species present in the reacting suspension were performed by means of a Shimadzu HPLC (Prominence LC-20A model and SPD-M20A Photodiode Array Detector), equipped with a Phenomenex Synergi 4 µm Hydro-RP 80A column at 313 K. Retention times and UV-vis spectra of the compounds were compared with those of standards (Sigma-Aldrich, purity ≥98%). The eluent consisted of 40% methanol and 60% deionised water. The flow rate was 0.2 cm³ min⁻¹.

Selectivity and conversion values were calculated as below:

$$\text{Selectivity}(\%) = [(\text{produced product moles}) / (\text{converted substrate moles})] \times 100;$$

$$\text{Conversion}(\%) = [(\text{reacted substrate moles}) / (\text{initial substrate moles})] \times 100$$

A specific photocatalytic run was carried out in order to produce a substantial amount of vitamin B₃. To this aim the run was performed with a 3-pyridinemethanol initial concentration of 10 mM and 0.2 g L⁻¹ of Pt-P25 at pH 12; this run lasted 10 h. The aldehyde present in the aqueous phase was extracted with ethyl acetate and then the aqueous phase was concentrated by a rotovapor apparatus. Vitamin B₃ was purified by column chromatography by using a mixture of methanol and ethyl acetate (2:1 v:v) as the mobile phase (69 mg, 37% yield).

The synthesized vitamin B₃ was purified and characterized by ¹H NMR analysis. The analysis data (δ (ppm, DMSO)): 7.55–7.58 (1H, ddd, J =8.0, 4.8 and 0.8 Hz), 8.27–8.31 (1H, dt, J =8.0 and 2.0 Hz), 8.80–8.82 (1H, dd, J =4.8 and 2.0 Hz), 9.09–9.10 (1H, dd, J =2.0 and 0.8 Hz), 13.45 (1H, s, COOH)) coincide with those of commercial vitamin B₃.

3. Results and discussion

3.1. Characterization

XRD patterns of P25 and HP TiO₂ photocatalysts are given in Fig. 1. The peaks assignable to anatase are those at 25.6°, 38.08°, 48.1° and 54.6° [6]. Those referring to rutile are at 27.5°, 36.5°, 41°,

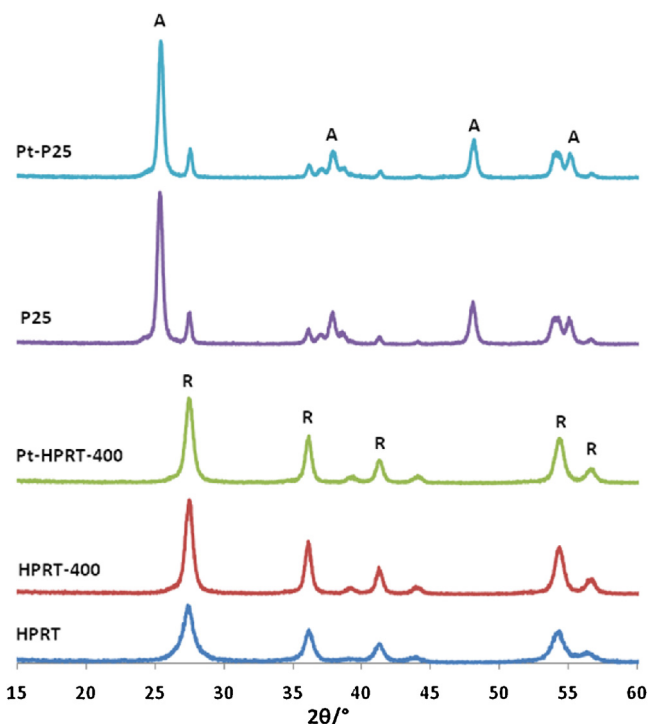


Fig. 1. XRD pattern of Pt-P25, P25, Pt-HPRT-400, HPRT-400 and HPRT.

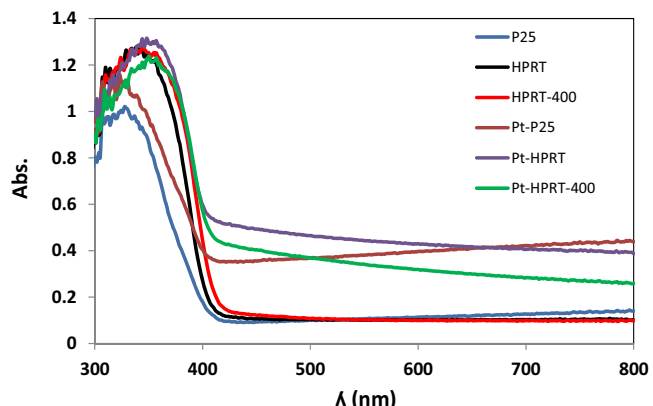
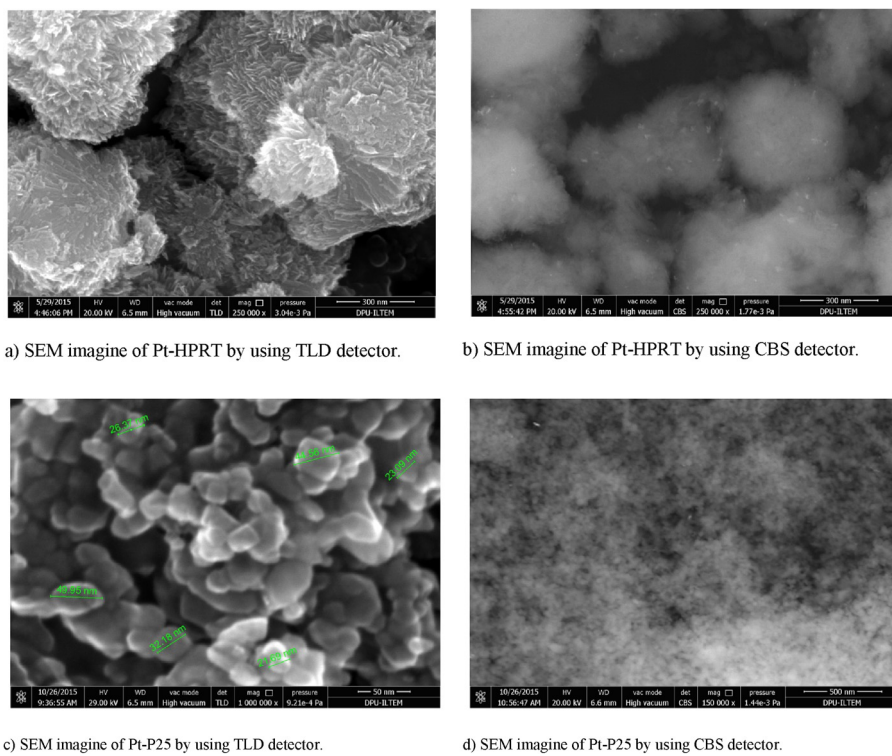


Fig. 2. UV-vis spectra of the pristine and Pt loaded home-prepared and commercial TiO₂ photocatalysts.

54.1° and 56.5° [6] and those referring to platinum are at 39.8°, 46.2° and 67.5° [21]. HPRT, HPRT-400 and Pt-HPRT-400 are in rutile phases and P25 and Pt-P25 are in anatase and rutile phases (A:80%, R:20%). Because Pt content of samples is very low, Pt peaks are not detected in the spectra of Fig. 1. Low temperature prepared samples (HPRT) are mainly amorphous, while the others are crystalline according to their broad and sharp XRD peaks, respectively.

UV-vis spectra of the pristine and Pt loaded TiO₂'s are reported in Fig. 2. The spectra show that all pristine samples have a strong absorbance in the UV region, until ca. 420 nm, while Pt loaded TiO₂ photocatalysts have good absorbance under visible irradiation, at least until 800 nm.

Crystalline phase, BET specific surface area (SSA) and crystallite size (calculated by using the Scherrer equation) of TiO₂ photocatalysts are reported in Table 2. Low temperature prepared catalysts (HPRT and Pt-HPRT) have high surface area and low crystallite sizes, while high temperature prepared ones have opposite features. Crystallite size of Pt-P25 is a little higher than that of P25.

Fig. 3. SEM imagines of pristine and Pt loaded TiO_2 photocatalysts.**Table 2**

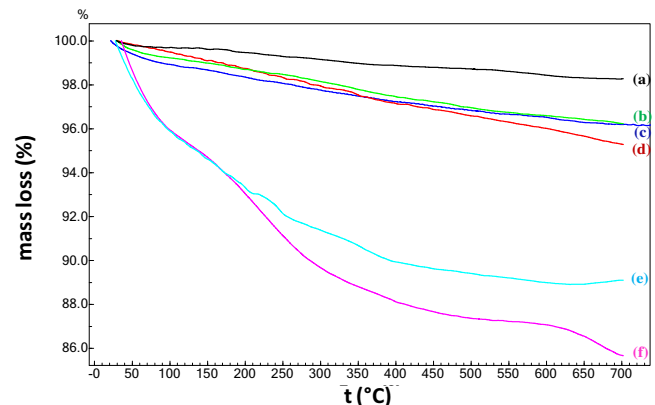
Crystalline phase, BET specific surface area (SSA) and crystallite size of TiO_2 photocatalysts.

Catalyst	Phase	SSA ($\text{m}^2 \text{g}^{-1}$)	Crystallite size (nm)
HPRT	rutile	105	7
Pt-HPRT	rutile	102	7
HPRT-400	rutile	46	12
Pt-HPRT-400	rutile	43	12
P25	anatase-rutile	63	18:20 (A:R)
Pt-P25	anatase-rutile	55	19:23 (A:R)

In addition, BET specific surface areas of loaded catalysts are little lesser than un-loaded ones. This situation could be due to the fact that Pt loading on the catalysts surface would cover defect sites and then determine the small decrease of surface area.

Fig. 3 reports SEM images of pristine and Pt loaded TiO_2 photocatalysts. The Pt-HPRT sample image (Fig. 3b) shows brilliant parts characteristic of deposited Pt, which are well distributed on the catalyst surface. SEM images of HPRT-400 and Pt-HPRT-400 (see Figs. S1a and S1b) are very similar; these samples are more crystalline than HPRT. By considering SEM images of P25 and Pt-P25 samples, Pt loading does not change significantly their morphology (Figs. 3 c and S1d). EDAX mapping of Pt-P25 confirms that Pt is well distributed (Fig. S1e).

TGA curves of all TiO_2 samples are showed in Fig. 4. These curves could be divided in three regions [20]. The region between 30 °C and 120 °C is indicative of the presence of physically adsorbed water ($\text{H}_2\text{O}_{\text{phys}}$); the regions between 120 °C and 300 °C and between 300 °C and 600 °C can be related to weakly (OH_{weak}) and strongly ($\text{OH}_{\text{strong}}$) bonded hydroxyl groups, respectively. The values of these hydroxyl amounts are reported as percentages (w/w) in Table 3. Total hydroxyl group amounts (OH_{total}) on TiO_2 surface are obtained by summing the OH_{weak} and $\text{OH}_{\text{strong}}$ values. All low temperature prepared samples have $\text{H}_2\text{O}_{\text{phys}}$, OH_{weak} and $\text{OH}_{\text{strong}}$ values very higher than those of high temperature prepared HP and commercial TiO_2 samples. For instance, OH_{total} values of badly

Fig. 4. TGA analysis results of well and badly crystallized TiO_2 photocatalysts. (a) Pt-HPRT-400, (b) Pt-P25, (c) P25, (d) HPRT-400, (e) Pt-HPRT, (f) HPRT.

crystalline samples are between 5.8% and 8.4%, while these values are only between 1.2% and 3.3% for crystalline TiO_2 samples. In addition, it is very interesting that Pt loaded HP TiO_2 samples have lesser $\text{H}_2\text{O}_{\text{phys}}$, OH_{weak} and $\text{OH}_{\text{strong}}$ percentages than those of un-loaded samples. This result obviously shows that metallic Pt loading decreases the hydroxyl amount on the TiO_2 surface for all HP TiO_2 photocatalysts. An opposite trend was observed for Degussa P25; according to XPS results (discussed below) in the Pt-P25 sample metal is in the cationic form (Pt^{2+}), while in the Pt-HPRT it is in metallic form (Pt^0).

Fig. 5 shows the XPS results of the main photoelectron peaks as binding energies of platinum ($\text{Pt}-4\text{f}_{5/2}$ and $\text{Pt}-4\text{f}_{7/2}$) of Pt loaded samples. Un-loaded TiO_2 (Degussa P25) was also used as a reference. The peak values of $\text{Pt}-4\text{f}_{7/2}$ and $\text{Pt}-4\text{f}_{5/2}$ at 70.7 and 74.0 eV, respectively, are attributed to Pt^0 and those at 72.3 and 75.7 eV to Pt^{2+} [22]. Therefore loaded Pt on Pt-HPRT-400 is mainly in metallic form; while that of Pt-P25 is mainly Pt^{2+} . This difference is probably

Table 3

The weight percentage (w/w) of physically adsorbed water (H_2O_{phys}), weakly (OH_{weak}) and strongly bonded hydroxyl (OH_{strong}) groups determined from TGA curves.

Sample	H_2O_{phys} [30–120 °C], (%)	OH_{weak} [120–300 °C], (%)	OH_{strong} [300–600 °C], (%)	OH_{total} [120–600 °C], (%)
HPRT	4.7	5.8	2.6	8.4
Pt-HPRT	4.4	4.0	2.4	6.4
HPRT-400	0.66	1.4	1.9	3.3
Pt-HPRT-400	0.31	0.54	0.71	1.3
P25	0.97	1.0	1.2	2.2
Pt-P25	0.87	0.99	1.6	2.6

Table 4

The names and structures of used alcohols and their corresponding aldehydes and acids.

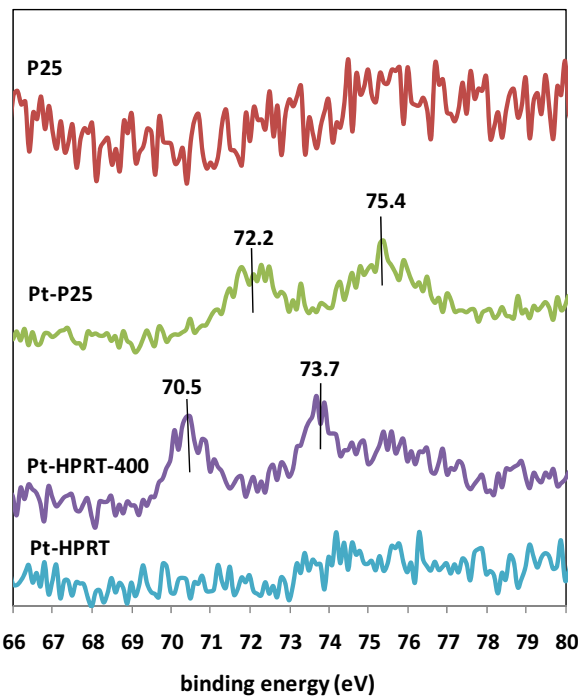
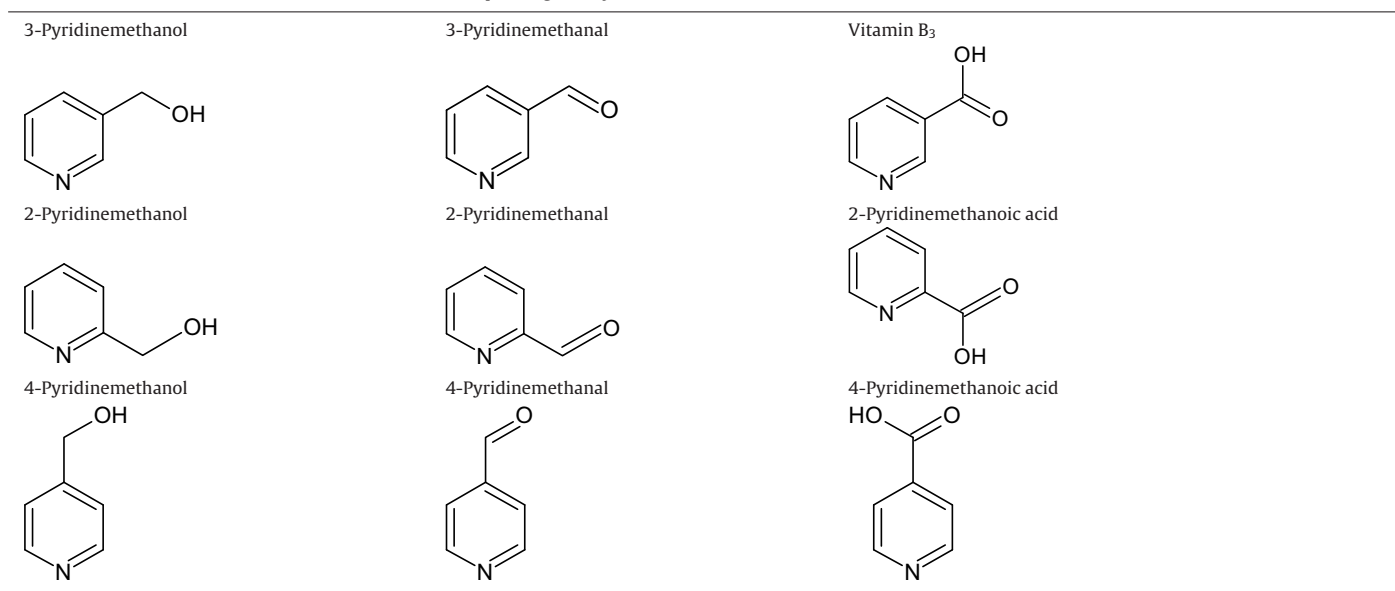
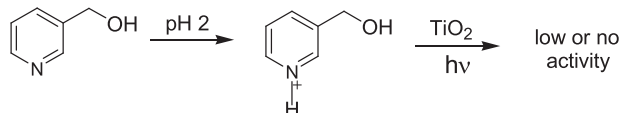


Fig. 5. Pt-4f XPS spectra of pristine and Pt loaded TiO_2 samples.

determined by the different calcination processes of Pt-HPRT-400 and Pt-P25. In fact HPRT-400 was prepared and then platinised, while Degussa P25 was platinised and then calcined at 400 °C.



Scheme 1. The hypothesized mechanism for the 3-pyridinemethanol oxidation at pH 2.

The peak values of Pt-HPRT are not clear, probably because the Pt species are spread out on the high surface of the support without forming aggregates which can be analysed by XPS (see Fig. 3b).

3.2. Photoreactivity

The names and structures of the used alcohols and their corresponding aldehydes and acids are given in Table 4.

Tables 5–8 show the experimental results of photocatalytic runs carried out at different experimental conditions. Table 5 reports the results for the oxidation of 3-pyridinemethanol performed under UV-vis irradiation at different pH's. This table gives the alcohol conversions for 3 h irradiation and the selectivities to aldehyde and acid for 15% conversion. Total selectivity to the corresponding aldehyde and acid is also given.

In homogenous conditions no reactivity was observed. In heterogeneous conditions, the best activity and total selectivity results were found at pH 7. At pH 2 no activity was found by using HPRT and HPRT-400, probably due to the fact that at this high acidity, nitrogen atom of 3-pyridinemethanol takes a proton and remains more stable (see Scheme 1) [23]. At this pH, however, Pt-P25 photocatalyst showed very low activity (12% conversion for 3 h) but high total selectivity (84%). These results show that the oxidative strength of

Table 5

The experimental results of photocatalytic oxidation of 3-pyridinemethanol performed under UV-vis irradiation.

Catalyst	pH	Conversion for 3 h irradiation	Aldehyde selectivity for 15% conv.	Vit. B ₃ select. for 15% conv.	Total select. for 15% conv.
Homogeneous	7	No activity			
HPRT	2	No activity			
HPRT-400	2	No activity			
HPRT	4	17	46	6	52
HPRT	7	29	63	9	72
HPRT	9.5	16	50	11	61
HPRT	12	17	38	31	69
Pt-HPRT	7	43	88	12	100
HPRT-400	7	15	70	8	78
Pt-HPRT-400	7	64	87	13	100
P25	7	48	48	9	57
Pt-P25	2	12	75	9	84
Pt-P25	7	47	70	11	81

Table 6

The experimental results of photocatalytic oxidation of 3-pyridinemethanol performed at different pH's under UV irradiation.

Catalyst	pH	Conversion for 3 h irradiation	Aldehyde selectivity for 15% conv.	Vitamin B ₃ selectivity for 15% conv.	Total selectivity for 15% conv.	Aldehyde selectivity for 50% conv.	Vitamin B ₃ selectivity for 50% conv.	Total selectivity for 50% conv.	t _{1/2} (min)
homogenous	7	No activity							
homogenous	12	No activity							
HPRT	7	61	73	14	87	52	26	78	130
HPRT	12	19	47	53	100	25	75	100	700
Pt-HPRT	7	57	80	20	100	56	26	82	120
Pt-HPRT	12	15	55	45	100	29	71	100	900
HPRT-400	7	10	84	16	100	70	30	100	1100
HPRT-400	12	14	70	30	100				
Pt-HPRT-400	7	64	92	8	100	74	21	95	100
Pt-HPRT-400	12	33	77	23	100	42	58	100	450
P25	7	83	40	8	48	33	11	44	60
P25	12	94	51	41	92	34	43	77	50
Pt-P25	7	75	70	14	84	50	16	66	65
Pt-P25	12	88	62	36	98	39	47	86	60

Table 7

The experimental results of photocatalytic oxidation of 3-pyridinemethanol performed under visible irradiation at pH 7.

Catalyst	Conversion for 3 h irradiation	Aldehyde selectivity for 5% conv.	Acid selectivity for 5% conv.	Total selectivity for 5% conv.	t _{1/2} (min)
Homogeneous	No activity				
HPRT	3				
Pt-HPRT	8	91	9	100	
HPRT-400	2				
Pt-HPRT-400	54	92	8	100	
P25	6	66	6	72	155
Pt-P25	12	58	10	68	

Table 8

The experimental results of photocatalytic oxidation of 4-pyridinemethanol performed under UV irradiation at pH 7.

Catalyst	Conversion for 3 h irradiation	Aldehyde selectivity for 15% conv.	Acid selectivity for 15% conv.	Total selectivity for 15% conv.	Aldehyde selectivity for 50% conv.	Acid selectivity for 50% conv.	Total selectivity for 50% conv.	t _{1/2} (min)
Homogeneous	No activity							
HPRT	54	66	27	93	27	37	64	140
HPRT-400	14	74	26	100				
Pt-HPRT-400	62	85	15	100	57	32	89	120
P25	97	35	14	49	26	13	39	40
Pt-P25	82	62	17	79	42	18	60	70

HPRT and HPRT-400 is not enough to oxidise 3-pyridinemethanol at pH 2, while that of Pt-P25 is enough.

The highest vitamin B₃ selectivity was obtained at pH 12 (31%, 3–4 fold higher than that at other pH's) and at this pH total selectivity is very close to that at pH 7 (72% vs. 69%). In other words, the formation of corresponding aldehyde is favoured at neutral conditions, while in basic conditions that of the corresponding acid (vitamin B₃). The first oxidation product of 3-pyridinemethanol is

3-pyridinemethanal and the second one is vitamin B₃. Probably, in basic conditions, the aldehyde transforms easily to vitamin B₃ [23].

P25 and Pt-P25 were also used for the same reaction at pH 7 (Table 5). The activity of P25 and Pt-P25 are similar, however aldehyde selectivity increases by Pt loading from 48% to 70%. This result shows that Pt loading on P25 has favourable effects on the selectivity; it could be due to the fact that Pt loading modifies the TiO₂ surface sites responsible of mineralization reaction and, moreover,

it generates new surface sites able to carry out partial oxidation reaction. Pt loaded HP samples (Pt-HPRT and Pt-HPRT-400) showed higher activity and total selectivity (100%) with respect to unloaded ones at pH 7 under UV-vis irradiation.

The work of Spasiano et al. [15] reports that the optimum pH was 2; in addition, by increasing pH from 1 to 4, both aldehyde and vitamin B₃ yields decreased. In the present work, at pH 2 no or low activity was observed (depending on used photocatalyst) and at neutral and strongly basic conditions very high vitamin B₃ selectivity was obtained. These differences probably depend on aerated or de-aerated conditions imposed to the photocatalytic system. Using O₂ from air as electron acceptor increases the reaction rate and in the poor acidic (pH 4), neutral (pH = 7) or basic (pH = 12) conditions high selectivity could be obtained. In Spasiano's work [15], nano zero valent copper (Cu(II) salts used as precursor) was adopted as cocatalyst on P25 for minimizing the electron-hole recombination in order to increase the activity. In that work the photocatalytic reaction was investigated until pH 4 while in our system the pH range is large and selectivity problem is overcome by using HP catalysts or Pt loading on TiO₂ surface.

Table 6 reports the experimental results of photocatalytic oxidation of 3-pyridinemethanol performed at pH 7 and 12 under UV irradiation. In this table the half-life times ($t_{1/2}$) and the selectivity values for 50% conversion are also given.

Under UV irradiation better activity and selectivity results are obtained with respect to those under UV-vis irradiation.

The conversions obtained at pH 7 are much higher than those at pH 12 for HPRT (61% vs. 19%) and Pt-HPRT (57% vs. 15%) photocatalysts. On the contrary, P25 and Pt-P25 show a little better activity at pH 12 than that at pH 7. Moreover, like the results of **Table 5**, at pH 12 higher vitamin B₃ selectivities were obtained with respect to those at pH 7.

Pt-HPRT shows a little less photoactivity than HPRT at pH 7 and 12; however, the HPRT total selectivity increases from 87% to 100% (for 15% conv.) at pH 7 by Pt loading. Moreover, at pH 12 100% total selectivity is obtained for both HPRT and Pt-HPRT catalysts.

The conversion of HPRT calcined sample (HPRT-400) drastically decreases from 61% to 10% (for 3 h irr.) at pH 7, probably due to different factors as the decrease of its surface area (105 vs. 46 m²/g) and surface hydroxyl group density (see **Table 3**) and the growth of crystallite sizes determined by calcination (7 vs. 12 nm) [5b,19]. Surface hydroxyl groups are the species able to adsorb O₂, which acts as electron acceptor and is a necessary reactant for photocatalytic oxidation [2].

It is very interesting that, differently from Pt-HPRT, Pt loading strongly affects the photoactivity of HPRT-400 sample at pH 7 and 12. For instance, HPRT-400 conversion increased from 10% to 64% for 3 h irradiation by Pt loading. In addition HPRT and Pt-HPRT-400 showed 100% total selectivity at both pH's for 15% conversion. These results show that very selective and complete 3-pyridinemethanol oxidation could be attainable by using Pt-HPRT-400 at neutral or basic conditions. Because the first and second 3-pyridinemethanol oxidation products are 3-pyridinemethanal and vitamin B₃, respectively, vitamin B₃/aldehyde ratio increases by increasing the conversion as it may be seen in **Table 6**. The highest vitamin B₃ selectivity was obtained with HPRT (75%) for 50% conversion even if the half-life time is very high (700 min). This reaction shows a zero order kinetics in the used experimental conditions (see **Fig. 8**). Pt-P25 showed better performances than those of P25 at pH 7 and 12. Loading Pt on P25 decreases the activity, differently from Pt-HPRT-400; however it increases significantly the selectivity at pH 7. It is very interesting that very fast (88% conv. for 3 h irr.) and selective (98% total select. for 15% conv.) photocatalytic oxidation of vitamin B₃ could be performed using Pt-P25 under UV irradiation at pH 12. HPRT is more selective catalyst than Pt-P25 for vitamin B₃

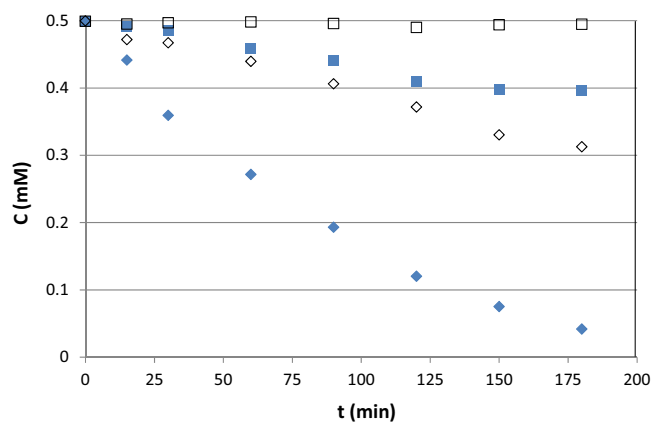


Fig. 6. Representative runs of photocatalytic oxidation of vitamin B₃ (performed at pH 12, empty symbols) and 2-pyridinemethanoic acid (performed at pH 7, full symbols) by using HPRT (□ and ■) and P25 (◊ and ♦) photocatalysts under UV irradiation.

production at pH 12; however HPRT shows very low photocatalytic activity than Pt-P25 (19% vs. 88% conversion for 3 h irradiation).

Fig. 6 shows the results of representative runs of photocatalytic oxidation of vitamin B₃ by using HPRT and P25 samples under UV irradiation at pH 12 (photocatalytic oxidation of 2-pyridinemethanoic acid will be discussed later). At this pH, there is no decomposition of vitamin B₃ by using HPRT, while P25 catalyst decomposes it. This experimental evidence explains why HPRT is more selective catalyst than P25. At pH 12, vitamin B₃ is more stable and the oxidative strength of HPRT is not enough to decompose it. 3-Pyridinemethanol conversion was 94% (see **Table 6**), while that of vitamin B₃ is 40% for 3 h irradiation at pH 12 under UV irradiation by using P25. This result shows that the stability of the product in the experimental conditions of the reactivity runs plays an important role in the selectivity.

Table 7 gives the experimental results of photocatalytic oxidation of 3-pyridinemethanol performed under visible irradiation at pH 7. Pt-HPRT-400 sample showed significant activity under visible irradiation; its conversion for 3 h irradiation was 54%, while the conversions obtained with the other samples were below 12%. The Pt-HPRT-400 total selectivity was 100% but the aldehyde selectivity was much higher than that of vitamin B₃ (92% vs. 8%).

Table 8 reports the experimental results of photocatalytic oxidation of 4-pyridinemethanol performed under UV irradiation at pH 7 using Pt loaded and pristine HPRT and P25 catalysts. HPRT showed high total selectivity (93% for 15% conv.) and alcohol conversion. The conversion with HPRT-400 drastically decreased with respect to HPRT, from 54% to 14% (for 3 h irr.). The Pt-HPRT-400 sample showed conversion ca. 4.4 fold higher (62% for 3 h irr.) than that of HPRT-400 and 100% total selectivity for 15% conversion. Therefore the catalytic properties of HPRT-400 were significantly improved by Pt loading. Pt loading on P25 shows different effects from those of HPRT-400; its activity decreased while the total selectivity increased significantly from 49% to 79% for 15% conversion.

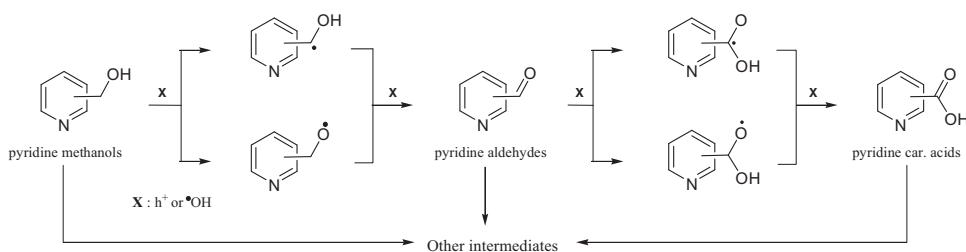
Table 9 reports the experimental results of photocatalytic oxidation of 2-pyridinemethanol performed under UV irradiation at pH 7. By considering both activity and selectivity results, HPRT and Pt-P25 showed the best performances for selective 2-pyridinemethanol oxidation. With respect to HPRT-400, Pt-HPRT-400 showed higher activity (27% vs. 56% conversion for 3 h irr.) and selectivity (87% vs. 100% for 15% conv.). With respect to P25, however, Pt-P25 showed less activity but higher total selectivity (67 vs. 49% for 15% conversion).

It is very interesting that by using commercial samples, negligible amount of corresponding 2-pyridinemethanoic acid was

Table 9

The experimental results of photocatalytic oxidation of 2-pyridinemethanol performed under UV irradiation at pH 7.

Catalyst	Conversion for 3 h irradiation	Aldehyde selectivity for 15% conv.	Acid selectivity for 15% conv.	Total selectivity for 15% conv.	Aldehyde selectivity for 50% conv.	Acid selectivity for 50% conv.	Total selectivity for 50% conv.	$t_{1/2}$ (min)
Homogeneous	No activity							
HPRT	74	32	68	100	8	34	42	75
HPRT-400	27	27	61	87				
Pt-HPRT-400	56	48	52	100	11	69	80	135
P25	87	48	1	49	27	4	31	50
Pt-P25	79	67	0	67	41	0	41	55



Scheme 2. The hypothesized mechanism for the pyridinemethanol oxidation to pyridine aldehydes and pyridine carboxylic acids.

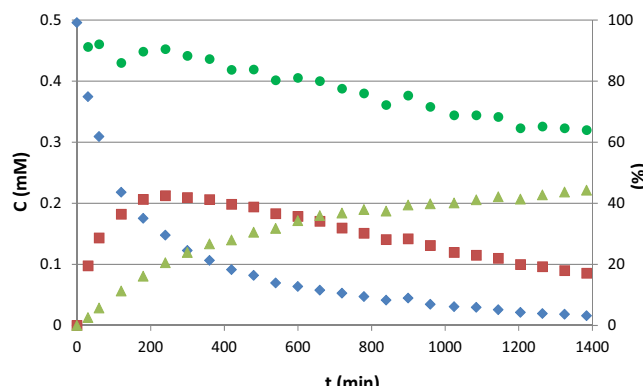


Fig. 7. A representative run of photocatalytic oxidation of 3-pyridinemethanol (◆) to corresponding aldehyde (■) and acid (vitamin B₃, ▲) using Pt-HPRT-400 at pH 7 and under UV irradiation. Total selectivity (●) is at right axis.

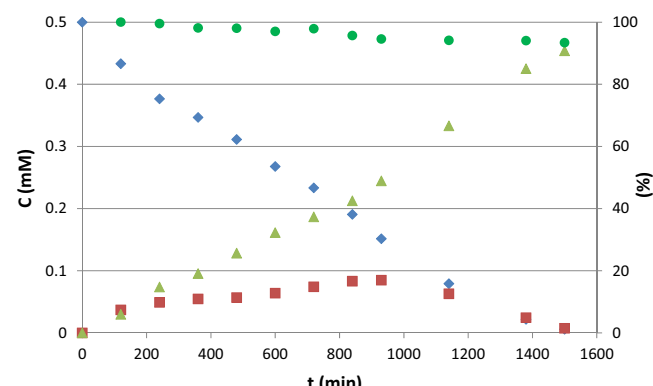


Fig. 8. A representative run of photocatalytic oxidation of 3-pyridinemethanol (◆) to corresponding aldehyde (■) and acid (vitamin B₃, ▲) using HPRT at pH 12 and under UV irradiation. Total selectivity (●) is at right axis.

obtained. This result could be due to the acid instability on P25 and Pt-P25 surface. These catalysts are very crystalline. Indeed, HPRT, a poor crystalline sample according to its broad XRD patterns, showed highest acid selectivity (68% for 15 conv.). The surface hydroxyl group density of P25 and Pt-P25 is lesser than that of HPRT, as indicated by their TGA results (see Fig. 4 and Table 3). In order to check this point, photocatalytic oxidation of 2-pyridinemethanoic acid has been performed by using P25 and HPRT (see Fig. 6). Indeed, by using P25 and HPRT, the conversions of 2-pyridinemethanoic acid at pH 7 and under UV irradiation are ca. 92% and 20%, respectively. Therefore, the results show that the produced 2-pyridinemethanoic acid easily decomposes on the crystalline TiO₂ surface.

In order to understand the effect of the nitrogen atom of aromatic ring on the reactivity, it is useful to compare the results obtained for the photocatalytic oxidation of pyridinemethanols and benzyl alcohol. In our previous works [5a–d], negligible benzoic acid selectivities were obtained (ca. 1%), while in this work, high selectivities of pyridinemethanoic acids were obtained. The obvious conclusion of these findings is that nitrogen atom in the aromatic ring increases the stability of pyridinemethanoic acids.

Fig. 7 shows a representative run of photocatalytic oxidation of 3-pyridinemethanol to corresponding aldehyde and acid (vitamin B₃) using Pt-HPRT-400 at pH 7 and under UV irradiation. In the

course of the run, alcohol concentration decreases while aldehyde and vitamin B₃ concentrations increase. Initially, aldehyde production rate is very high and it reaches a maximum; then it starts to decrease. On the contrary, the vitamin B₃ concentration continuously increases. This result clearly shows that a series reactions are occurring, the first oxidation product being aldehyde and the second one the corresponding acid. The total selectivity also decreases with time due to overoxidation products of aldehyde and vitamin B₃ [5].

Fig. 8 shows the results of a representative run of photocatalytic oxidation of 3-pyridinemethanol to corresponding aldehyde and vitamin B₃ using HPRT at pH 12 and under UV irradiation. The kinetics of substrate oxidation and acid production are zero order, being the acid production rate always very high, differently from that observed in Fig. 7. This is probably due to the fact that the transformation rate of aldehyde to acid is very high in basic condition [23]; 99% alcohol conversion with 92% vitamin B₃ selectivity was obtained.

A likely mechanism for the pyridinemethanol oxidation to pyridine aldehydes and pyridine carboxylic acids is hypothesized in Scheme 2. The initial steps may be the interaction of positive holes (h⁺) or hydroxyl radicals (•OH) with pyridinemethanol producing pyridine aldehydes which are subsequently oxidized to pyridine

carboxylic acids. Other intermediates, mainly broken-ring products, could be produced by over oxidation of these molecules.

4. Conclusions

Selective photocatalytic oxidation of 2, 3 and 4-pyridinemethanol to corresponding aldehydes and acids has been performed in water and aerated conditions using Pt loaded HP and commercial TiO₂ samples. TiO₂ photocatalysts in different crystal phase, particle size, crystallinity, specific surface area, and amount of surface hydroxyl groups were used for the synthesis reaction and the obtained results are compared each other. Pt loading, suspension pH and light source effects on the reactivity and selectivity were investigated. The influence of the ortho and para position of the benzylic group in pyridine was also studied. The highest vitamin B₃ selectivity (75%) for 50% conversion was found with HPRT at pH 12 and under UV irradiation. In a 24 h run carried out at the same conditions the vitamin B₃ yield was ca. 90%. The obtained results show that (i) in order to synthesize vitamin B₃ in green conditions, the photocatalyst should be poorly crystalline or Pt loaded; (ii) nitrogen atom in the aromatic ring increases the stability of pyridinemethanoic acids; (iii) the product stability in the experimental conditions plays an important role in the selectivity; (iv) Pt-HPRT-400 catalyst showed significant activity under visible irradiation and (v) pH is very important parameter for both activity and product selectivity.

Acknowledgements

Authors thank the Scientific Research Project Council of Afyon Kocatepe University (BAP project no:16.KARIYER.08) for financial support and Prof. Leonardo Palmisano (Palermo University, Italy) for his useful suggestions.

Appendix A. Supplementary data

Supplementary data associated with this article can be found, in the online version, at <http://dx.doi.org/10.1016/j.apcatb.2016.09.063>.

References

- [1] P. Anastas, N. Eghbali, Chem. Soc. Rev. 39 (2010) 301–312.
- [2] (a) M. Schiavello (Ed.), *Heterogeneous Photocatalysis*, Wiley, Chichester, 1997;
 (b) V. Augugliaro, M. Bellardita, V. Loddo, G. Palmisano, L. Palmisano, S. Yurdakal, J. Photochem. Photobiol. C: Photochem. Rev. 13 (2012) 224–245;
 (c) D. Spasiano, R. Marotta, S. Malato, P. Fernandez-Ibañez, I. Di Somma, Appl. Catal. B: Environ. 170–171 (2015) 90–123.
- [3] R.A. Sheldon, Catal. Today 247 (2015) 4–13.
- [4] (a) L. Palmisano, V. Augugliaro, M. Bellardita, A. Di Paola, E. García López, V. Loddo, G. Marci, G. Palmisano, S. Yurdakal, ChemSusChem 4 (2011) 1431–1438;
 (b) V. Augugliaro, G. Camera-Roda, V. Loddo, G. Palmisano, L. Palmisano, J. Soria, S. Yurdakal, J. Phys. Chem. Lett. 6 (2015) 1968–1981.
- [5] (a) S. Yurdakal, G. Palmisano, V. Loddo, V. Augugliaro, L. Palmisano, J. Am. Chem. Soc. 130 (2008) 1568–1569;
 (b) S. Yurdakal, G. Palmisano, V. Loddo, O. Alagöz, V. Augugliaro, L. Palmisano, Green Chem. 11 (2009) 510–516;
 (c) K. Sivarjanji, C. Gopinath, J. Mater. Chem. 21 (2011) 2639–2647.
- [6] S. Yurdakal, B.S. Tek, O. Alagöz, V. Augugliaro, V. Loddo, G. Palmisano, L. Palmisano, ACS Sust. Chem. Eng. 1 (2013) 456–461.
- [7] N. Li, X. Lang, W. Ma, H. Ji, C. Chen, J. Zhao, Chem. Commun. 49 (2013) 5034–5036.
- [8] M. Bellardita, V. Loddo, G. Palmisano, I. Pipiri, L. Palmisano, V. Augugliaro, Appl. Catal. B: Environ. 144 (2014) 607–613.
- [9] V. Augugliaro, G. Camera Roda, V. Loddo, G. Palmisano, L. Palmisano, F. Parrino, M.A. Puma, Appl. Catal. B: Environ. 111–112 (2012) 555–561.
- [10] (a) V. Maurino, A. Bedini, M. Minella, F. Rubertelli, E. Pelizzetti, C. Minero, J. Adv. Oxid. Technol. 11 (2008) 184–192;
 (b) V. Augugliaro, H.H. El Nazer, V. Loddo, A. Mele, G. Palmisano, L. Palmisano, S. Yurdakal, Catal. Today 151 (2010) 21–28;
 (c) C. Minero, A. Bedini, V. Maurino, Appl. Catal. B: Environ. 128 (2012) 135–143.
- [11] B. Ohtani, B. Pal, S. Ikeda, Catal. Surv. Asia 7 (2003) 165–176.
- [12] (a) M.S. Hamdy, W.H. Saputera, E.J. Groenen, G. Mul, J. Catal. 310 (2014) 75–83;
 (b) B.-L. An, Y.-H. Fu, F.-Z. Dai, J.-Q. Xu, J. Alloy. Comp. 622 (2015) 426–431;
 (c) E. Kowalska, O.O.P. Mahaney, R. Abe, B. Ohtani, Phys. Chem. Chem. Phys. 12 (2010) 2344–2355;
- [13] (d) A. Bumajdad, M. Madkour, Phys. Chem. Chem. Phys. 16 (2014) 7146–7158;
 (e) X. Lang, X. Chen, J. Zhao, Chem. Soc. Rev. 43 (2014) 473–486.
- [14] (a) T. Morikawa, T. Ohwaki, K.I. Suzuki, S. Moribe, S. Tero-Kubota, Appl. Catal. B Environ. 83 (2008) 56–62;
 (b) E. Grabowska, J. Reszczynska, A. Zaleska, Water Res. 46 (2012) 5453–5471;
 (c) W. Kim, T. Tachikawa, H. Kim, N. Lakshminarayanan, P. Murugan, H. Park, T. Majima, W. Choi, Appl. Catal. B: Environ. 147 (2014) 642–650.
- [15] (a) H. Hirakawa, Y. Shiraishi, H. Sakamoto, S. Ichikawa, S. Tanaka, T. Hirai, Chem. Commun. 51 (2015) 2294–2297;
 (b) Y. Shiraishi, H. Sakamoto, Y. Sugano, S. Ichikawa, T. Hirai, ACS Nano 7 (2013) 9287–9297;
 (c) Y. Shiraishi, H. Sakamoto, K. Fujiwara, S. Ichikawa, T. Hirai, ACS Catal. 4 (2014) 2418–2425.
- [16] D. Spasiano, R. Marotta, I. Di Somma, G. Mancini, Appl. Catal. B: Environ. 163 (2015) 248–257.
- [17] M. Alfe, D. Spasiano, V. Gargiulo, G. Vitiello, R. Di Capua, R. Marotta, Appl. Catal. A: Gen. 487 (2014) 91–99.
- [18] D. Spasiano, L. Raspollini, S. Satyro, G. Mancini, F. Pirozzi, R. Marotta, Chem. Eng. J. 283 (2016) 1176–1186.
- [19] T. Ohno, T. Tsubota, R. Inaba, J. Appl. Electrochem. 35 (2015) 783–791.
- [20] S. Yurdakal, B.S. Tek, Ç. Değirmenç, G. Palmisano, Catal. Today (2016) <http://dx.doi.org/10.1016/j.cattod.2016.05.054>.
- [21] B.S. Tek, S. Yurdakal, L. Özcan, V. Augugliaro, V. Loddo, G. Palmisano, Sci. Adv. Mater. 7 (2015) 2306–2319.
- [22] L. Wang, W. Xu, X. Wu, Q. Li, Z. Wang, X. Zheng, J. Nanomater. (2014), Article ID: 401617.
- [23] (a) E.A. Kozlova, T.P. Lyubina, M.A. Nasalevich, A.V. Vorontsov, A.V. Miller, V.V. Kaichev, V.N. Parmon, Catal. Commun. 12 (2011) 597–601;
 (b) H. Sun, G. Zhou, S. Liu, H.M. Ang, M.O. Tadé, S. Wang, Chem. Eng. J. 231 (2013) 18–25;
 (c) Z. Wu, Z. Shenga, Y. Liu, H. Wang, J. Mo, J. Hazard. Mater. 185 (2011) 1053–1058.
- [24] A. Katritzky, C.A. Ramsden, J. Joule, *Handbook of Heterocyclic Chemistry*, 3rd ed., Elsevier, Amsterdam, 2010.